

# Internal Jugular Vein Compression Collar Mitigates Histopathological Alterations after Closed Head Rotational Head Impact in Swine: A Pilot Study

Rebekah Mannix,<sup>a,b,\*</sup> Nicholas J. Morriss,<sup>a</sup> Grace M. Conley,<sup>a</sup> William P. Meehan, III<sup>b,c,d,e</sup> Arthur Nedder,<sup>i</sup> Jianhua Qiu,<sup>a,d</sup> Jamison Float,<sup>f</sup> Christopher A. DiCesare<sup>f</sup> and Gregory D. Myer<sup>e,f,g,h</sup>

<sup>a</sup> Division of Emergency Medicine, Boston Children's Hospital, United States

<sup>b</sup> Harvard Medical School, United States

<sup>c</sup> Department of Orthopedics, Boston Children's Hospital, United States

<sup>d</sup> Department of Pediatrics, Boston Children's Hospital, United States

<sup>e</sup> Micheli Center for Sports Injury Prevention, United States

<sup>f</sup> Priority Designs, Columbus, OH, United States

<sup>g</sup> The SPORT Center, Division of Sports Medicine, Cincinnati Children's Hospital Medical Center, Cincinnati, OH, United States

<sup>h</sup> Departments of Pediatrics and Orthopaedic Surgery, College of Medicine, University of Cincinnati, Cincinnati, OH, United States

<sup>i</sup> DVM. Animal Resources Children's Hospital, Boston Children's Hospital, Boston, Massachusetts, USA

**Abstract**—Recently, there has been increased concern about microstructural brain changes after head trauma. Clinical studies have investigated a neck collar that applies gentle bilateral jugular vein compression, designed to increase intracranial blood volume and brain stiffness during head trauma, which neuroimaging has shown to result in a reduction in brain microstructural alterations after a season of American football and soccer. Here, we utilized a swine model of mild traumatic brain injury to investigate the effects of internal jugular vein (IJV) compression on histopathological outcomes after injury. Animals were randomized to collar treatment ( $n = 8$ ) or non-collar treatment ( $n = 6$ ), anesthetized and suspended such that the head was supported by breakable tape. A custom-built device was used to impact the head, thus allowing the head to break the tape and rotate along the sagittal plane. Accelerometer data were collected for each group. Sham injured animals ( $n = 2$ ) were exposed to anesthesia only. Following single head trauma, animals were euthanized and brains collected for histology. Whole slide immunohistochemistry was analyzed using Qupath software. There was no difference in linear or rotational acceleration between injured collar and non-collar animals ( $p > 0.05$ ). Injured animals demonstrated higher levels of the phosphorylated tau epitope AT8 ( $p < 0.05$ ) and the inflammatory microglial marker IBA1 ( $p < 0.05$ ) across the entire brain, but the effect of injury was markedly reduced by collar treatment ( $p < 0.05$ ). The current results indicate that internal jugular venous compression protects against histopathological alterations related to closed head trauma exposure. © 2020 IBRO. Published by Elsevier Ltd. All rights reserved.

**Key words:** mild traumatic brain injury, immunohistochemistry, phosphorylated tau.

## INTRODUCTION

The public health burden of head trauma resulting in mild traumatic brain injury (mTBI), including concussion, is enormous with millions of cases reported each year.

\*Correspondence to: Rebekah Mannix, Boston Children's Hospital, Division of Emergency Medicine, 300 Longwood Avenue, Boston, MA 02115, United States. Tel: +1-617-355-6624.

E-mail address: [Rebekah.Mannix@childrens.harvard.edu](mailto:Rebekah.Mannix@childrens.harvard.edu) (R. Mannix).

**Abbreviations:** CTE, chronic traumatic encephalopathy; IJV, internal jugular vein; mTBI, mild traumatic brain injury; PBS, phosphate buffered saline; WM, white matter.

The scientific community, as well as the public at large, now recognizes that the term “mild” is quite misleading, since as many as 30% of patients remain symptomatic one month after injury (Zemek et al., 2016). In addition, an increasing number of reports suggest a link exposure to head trauma, even those without overt clinical symptomatology (sometimes called subconcussive injury), to structural and histopathological changes in the brain (Koerte et al., 2012; Yuan et al., 2017; Myer et al., 2018; Yuan et al., 2018a; Schneider et al., 2019). Exposure to head trauma has been associated with long-term neurologic sequelae such as Alzheimer's Disease,

seizure disorder, multiple sclerosis and chronic traumatic encephalopathy (CTE) (Omalu et al., 2005, 2006; McKee et al., 2009; Stern et al., 2011; McKee et al., 2013; Noy et al., 2016; Mez et al., 2017). To date, there are no proven interventions to prevent or mitigate brain injury from head trauma.

The extent and severity of brain injury after head trauma is hypothesized to depend upon local brain deformation or strain, which may or may not result in overt clinical symptomatology and a subsequent ‘concussion’ diagnosis (Margulies and Coats, 2013). Micro-damage to the local tissue occurs when the magnitude or strain rate exceeds tissue mechanical properties. External head protection, including helmets (Schneider et al., 2017), does not fully mitigate the shear/strain energy absorption the brain undergoes during traumatic impacts. A key knowledge gap in prevention of brain injury is how to efficiently and effectively minimize movement of the brain through the cerebrospinal fluid inside of the skull (‘slosh’) to ameliorate differential acceleration between the skull and its contents (Benson et al., 2009).

To address this knowledge gap, several preliminary studies evaluating the use of an innovative compression collar applied to the jugular vein to increase cerebral blood volume as a means of protecting against mechanical slosh upon head impact have been reported (Yuan et al., 2017; 2018a,b). The published data indicate the potential to reduce neurophysiologic and microstructural brain alterations in response to head impacts using a jugular vein compression collar, fashioned off of the diagnostic Queckenstedt maneuver (Gilland et al., 1969; Myer et al., 2016a,b; 2018). Early small animal preclinical studies to date also reveal that jugular vein compression reduces a widely accepted marker of TBI—amyloid precursor protein-positive axons—by 83% during a 900 g impact protocol (Smith et al., 2012). Further, using the same impact protocol in a related preclinical TBI model, there was a greater than 45% reduction in degenerative neurons, reactive astrocytes, and microglial activation with the application of jugular vein impedance (Turner et al., 2012). However, these murine models lack the substantial white matter (WM) domains and specific pathophysiological features of human TBI, which may be key factors in the development of specific features of trauma-induced neuropathology.

In clinical studies, initial evidence indicates that imaging biomarkers of microstructural changes in WM after a season of head impact exposure is mitigated in athletes wearing a jugular venous compression collar compared to those not wearing a collar (Myer et al., 2016a,b; 2018). However, the prior clinical studies were unable to provide a direct measurement of brain microstructure to determine the protective benefits of jugular compression during head impact exposure and it is not clear how the protective effects on histopathology outcomes in murine models translates to the gyrencephalic brain. Thus, while evidence from clinical studies using imaging biomarkers and preclinical murine models to date are encouraging, further understanding of tissue level protection of jugular venous compression is needed.

For the current project, we have developed a closed head rotational head impact protocol in swine that provides the advantages of a more realistic impact blow with the ability to allow free movement of the head post-impact and imparting a rotational component to the brain throughout, approximating the environment that athletes are subjected to during competitive play. Our hypothesis to be tested is that jugular (i.e., neck) vein compression applied during head impact exposure and the resultant cerebral venous engorgement will reduce alterations in histological biomarkers of brain microstructure in response to single head impact exposure in large animal model.

## EXPERIMENTAL PROCEDURES

All animal experiments were conducted in accordance with protocols approved by Boston Children’s Hospital Institutional Animal Care and Use Committee and in accordance with the NIH Guide for the Care and Use of Laboratory Animals.

### Collar design

The swine collar was designed to occlude the jugular vein and be applied to an anesthetized swine, in a downward facing position. Due to the variability in swine neck size and geometry, the collar was designed with multiple adjustments to ensure proper occlusion of the IJV. During fittings, the IJV pods were opened to allow the collar to slip around the neck. Then, the IJV pod angle and lateral spacing were adjusted and locked into position so that the pods lied directly over the IJV. The adjustable neck pod was then tightened to provide proper pressure and occlusion of the IJV. The construction of the collar is a stainless-steel frame with 3D printed center structure, 3D printed IJV compression pod and 3D printed neck adjustment (Fig. 1).

### Head impact measurement

Each animal was fitted with an X Patch Pro accelerometer (X2 Biosystems; Seattle, Washington). The X Patch Pro is a small, durable device that attaches to the back of the neck behind the ear using an adhesive and tracked head accelerations due to impacts. The data recorded by the X Patch Pro was used in the final analysis to normalize the acceleration exposure between animals.

### Closed head injury

Six-month-old castrated male Yucatan miniature swine ( $n = 16$ ) were used for this study. A subset of 14 ( $n = 8$  collar and 6 non-collar) were subjected to a closed head impact concussion model. Sham animals ( $n = 2$ ) were subjected to anesthesia only. Sample size estimates were based on a prior mTBI swine study (Browne et al., 2011). Swine were anesthetized with telazol 2.2–6.6 mg/kg, xylazine 1.1–2.2 mg/kg and atropine 0.04 mg/kg and vital signs (heart rate, respiratory rate, pulse oximetry and core body temperature) were monitored throughout the procedure. After inductions, anesthetized swine were

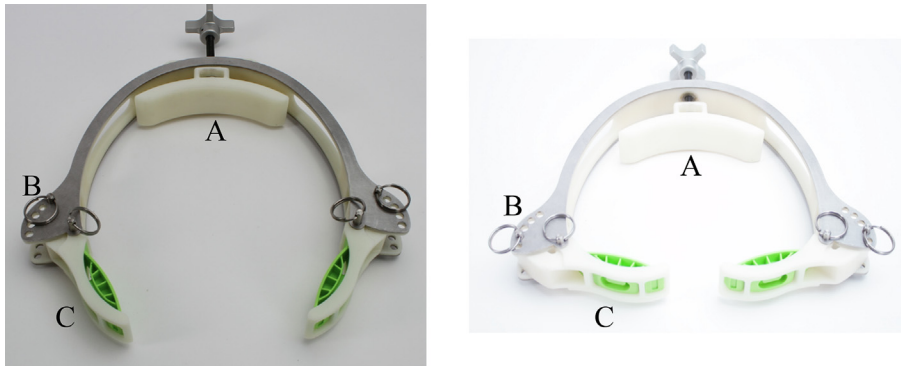


**Fig. 1.** Jugular compression collar worn by pigs. Images are labeled as follows. **(A)** Adjustable neck brace to adjust for varying neck sizes. **(B)** Pins to adjust the IJV pads at varying angles, allowing for different neck sizes. **(C)** IJV pads for venous compression. Left image shows IJV pads at most open position, as is used to place collar on pig necks. Right image shows IJV pads in the closed position providing venous compression.

placed in a modified Panepinto sling (Morgantown, West Virginia) attached to an impact device. Animals were randomly assigned to collar intervention and placed in a collar as above if assigned to collar treatment. Similar to testing in prior clinical trials, visual evidence of superior venous dilation was confirmed with ultrasound following neck collar application to the swine (Fig. 2). The head of collar and non-collar animals was cradled in a thin membrane held in position parallel to the floor. The impact device was positioned to make impact in a midline site, delineated by the intersection of two lines drawn from the medial aspect of each ear flap to the contralateral medial canthus of the eye. The midline between the nasofrontal and frontal parietal sutures. The impactor device

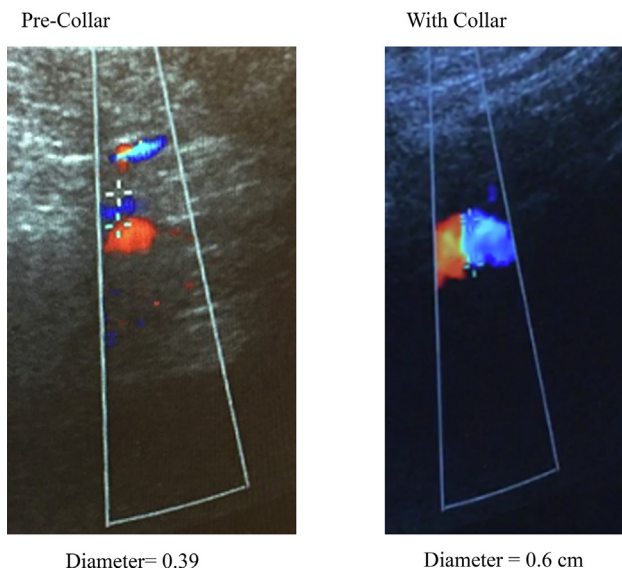


**Fig. 2.** Doppler ultrasound images of pig jugular vein without (left) and with (right) jugular compression collar. The image during collar was taken on the side of the collar proximal to the head, and as such the jugular vein (blue) is enlarged indicating reduced venous return from the head. Width of jugular vein as measured by the distance between markers on ultrasound is reported. (For interpretation of the references to color in this figure legend, the reader is referred to the web version of this article.)

was set at a 35 degree angle (1.5 m height from the head of the swine) and with a 15.9 kg total weight of the impactor arm. These parameters were a priori calculated to deliver a total gforce of  $\sim 120$  g, in the middle of the range reported in the clinical literature (Guskiewicz and Mihalik, 2011). Gforce calculations were made based on 15.9 kg weight of the impactor, 1.5 m height of the drop and 0.2 m deceleration distance after impact. Once set in position, the release lever was pressed and injury was delivered in the specified region of the skull, resulting in rotational acceleration of the head through the thin membrane. Rotational kinematics

were recorded using X-Patch Pro v1.1 (X2 Biosystems, Seattle WA) mounted to the neck and ear area on the swine and recorded running X2 XPP Lab Tool software (1600 Hz sampling rate). Heart rate, respiratory rate, oxygen saturation and temperature were measured during the injury procedure. Animals were allowed to recover in their cages.

#### Clinical behavior score

Based on routine post-procedure assessments by veterinary staff in our large animal facility, a clinical behavior score was devised to assess functional status after injury. A subset of animals ( $n = 4$ ) was monitored for baseline prior to injury and for five days after injury. The score was comprised of the following seven measures: strength, balance, coordination, activity level, latency to upright, reflexes, appetite, and urine/fecal output. Scoring for each measure was conducted as follows: A score of 5 constituted normal behavior (full response/activity/appetite/output); a score of 4 constituted a marginal decrement from normal behavior (little less than full response/activity/appetite/output); a score of 3 constituted a moderate decrement from normal behavior (responsive/active, but decreased/appetite & output altered); a score of 2 constituted a severe decrement from normal behavior (responds, but barely reacts/appetite & output decreased); a score of 1 constituted the near absence of normal behavior (barely responsive/appetite & output minimal); a score of 0 constituted the absence of normal behavior (no response, appetite, or output) In addition, pupillary response, ability to stand upright and the absence of vomiting were scored yes/no. The behavior score was implemented by veterinary technicians blinded to injury status. Results are reported as percent deviation from baseline score: difference between score on that day and baseline score, divided by baseline score, multiplied by 100 percent.

#### Animal euthanasia and tissue processing

Animals were euthanized 3–5 days after injury ( $n = 2$ –6/group) and 23 days post injury ( $n = 2$ /group) and all

subsequent analyses were adjusted for time from injury. Swine were anesthetized with telazol 2.2–6.6 mg/kg and xylazine 1.1–2.2 mg/kg and injected with lithium heparin (200 units/kg) intracardially to prevent blood clotting. Animals were then euthanized using intracardial Fatal Plus (110 mg/kg) and the brains were immediately removed and weighed. Brain tissue was placed in 4% paraformaldehyde upon removal and stored at 4 °C for approximately 2 weeks, after which they were placed in phosphate buffered saline (pH = 7.4) until sectioning. Brains were initially sectioned into 5 mm thick sections using a brain slicing matrix (Zivic Instruments, Pittsburgh PA). Five sections were then selected for further processing, starting at 20 mm from the front of the brain and alternating sections. This approach allowed for processing a representative range of brain regions from each brain. The selected sections were sent to Cummings Veterinary Medical Center Pathology Services for sectioning and immunohistochemistry.

### Sectioning and immunohistochemistry

Sections were bisected longitudinally and embedded into paraffin, from which 4- $\mu$ m slices were cut and mounted onto positively charged slides. Sections were baked at 65 °C for 30–60 min, deparaffinized, and hydrated to deionized water. Antigen retrieval was done: the slides were incubated in a 1:10 solution of Citrate Antigen Retrieval solution (Cell Marque, Declare) in deionized water, cooked in a steamer for 20 min and then allowed to cool for 20 min. Slides were twice rinsed in deionized water, and the following steps were conducted at room temperature. Slides were incubated in 3% aqueous hydrogen peroxide twice for 5 min each, in order to oxidize blood vessels and reduce false positives on immunohistochemistry. Slides were washed once in phosphate buffered saline (PBS) (pH = 7.4) and placed into an automatic slide stainer (BioGenix, i6000 system). This ensured that all slides were exposed to the same solutions of antibodies for the same duration, allowing comparison between slides. Slides were exposed to one of the following concentrations of primary antibodies for 30 min: AT8 at 5  $\mu$ g/ml (Thermo Scientific, MN1020) or IBA1 at 250 ng/ml (Wako Chemicals, 019-19741). Slides were then rinsed five times in PBS, incubated for 10 minutes in linking solution (Hi-Def Detection Kit, Cell Marque 954D-30), rinsed five times in PBS and incubated for 10 minutes in labeling solution (Hi-Def Detection Kit, Cell Marque 954D-30). Slides were rinsed five times in PBS and incubated in DAB Chromogen (Cell Marque, 957D-40) for 6 minutes, rinsed 5 times in PBS and counterstained with hematoxylin as follows: dipped three times in hematoxylin, rinsed three times in tap water, dipped 10 times in bluing reagent (4% ammonium hydroxide) and rinsed three times again in tap water. Slides were then dehydrated using increasing concentrations of ethanol and coverslipped.

### Automated histopathology

Automated, whole brain histopathology was employed for all histopathological outcomes, which we have previously

demonstrate correlate with manual cell counts (Morriss et al., 2020 *in press*). All slides were scanned using a ZEISS Axio Scan.Z1 automatic slide scanner located at the Harvard Center for Biological Imaging (Cambridge, MA), converted to a .czi file for each slide scanned, then analyzed using QuPath freeware v0.2.02 (<https://QuPath.github.io/>).

QuPath image analysis was deployed as follows, using code previously developed in our laboratory (see [Supplementary Information](#)). First, simple tissue detection created annotations around tissue located on the slide, and then automatically shrunk these annotations by 250  $\mu$ m from each border in order to exclude potential false positives along the edges of tissue (to exclude some areas of folded tissue, which would double the DAB signal of pixels in that area). Each slide was then manually rechecked for correct tissue identifications. Next, the QuPath code analyzed each image, exported the data in a text file to a previously determined folder, generated a “heat-map” that visualized stain intensity across the entire image, and exported the image of that heat-map. Finally, data for each slide were exported to excel for further analysis.

Quantification was accomplished using superpixels rather than cell-based procedures. Pixel-level quantification results in nearly identical methods across stains, allows for the capture of subcellular-level data that might be missed if cell-body based analysis were used, and also permits sensitivity analyses for different thresholds of positivity. For each image of a slide, QuPath iterated over all pixels in each image and grouped adjacent and similar pixels into superpixels of a set size (set at 50  $\mu$ m<sup>2</sup> to maximize resolution and processing speed). Pixel similarity was determined by their red-green-blue (RGB) values, which determined color and shade of the pixel. Positivity of each superpixel was determined at multiple different thresholds to allow for visualization of subcellular elements and perform sensitivity analyses of multiple thresholds. The use of multiple thresholds for positivity in the analysis of AT8 allowed distinct quantification and analysis of different significant cellular features. The lowermost threshold 1+ captured only subtly positive elements such as axons positive for tau, while middle threshold 2+ captured notably positive cell bodies, and uppermost threshold 3+ captured exclusively supercellular tau tangles or masses of strongly positive cells. For IBA1, the multiple thresholds allowed analysis that ranged from highly sensitive to highly specific. As IBA1 is present in non-activated microglia as well as activated, and the distinction between the two relies on the increased size of the cell body and number of microprocesses it was necessary to ensure that this increase could be seen across multiple thresholds.

### Generation of heat-maps

In order to visualize the distribution of DAB stains, we generated heatmaps of staining intensity for each image. QuPath allows the user to generate this visualization after quantified analysis in the form of heatmaps, applying a gradient of color to each

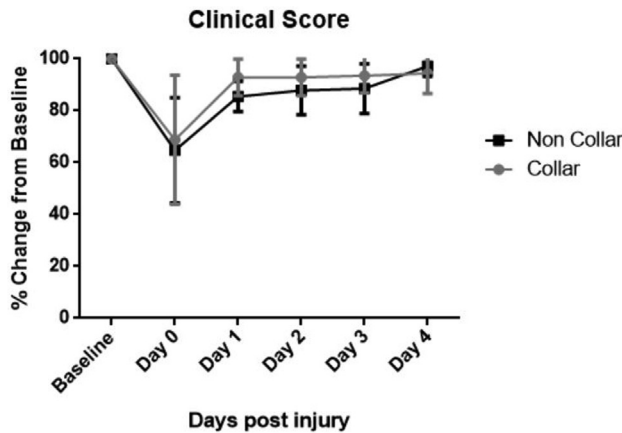


**Fig. 3.** Clinical symptom score for the five days after injury composed of the following eight measures: strength, balance, coordination, activity level, latency to upright, reflexes, appetite, and urine/fecal output. Data are presented as percent deviation from baseline score, with error bars representing standard deviation of two independent raters blinded to injury and collar status.

superpixel based on DAB intensity. This permits an easy qualitative analysis of the stained tissue and can be used to isolate regions of interest for complementary analyses.

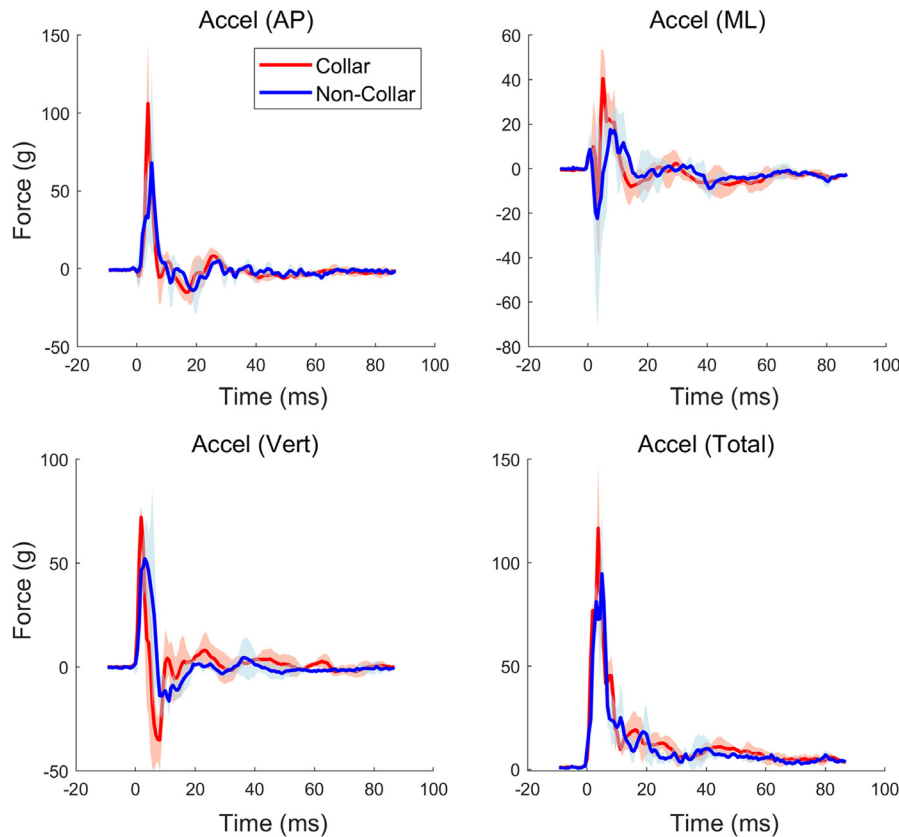


**Fig. 4.** Graphical display of time series data for accelerometry recorded for (mean  $\pm$  1 SE) linear acceleration and rotation velocity time series by group for all three axes of motion [anterior/posterior (AP), medial/lateral (ML), vertical (Vert)] and summated (Total) accelerations and velocities (final column). Visualized overlapping SEs over the time series indicate non-significant between group differences in head impact accelerations. Peak values for summated (Total) values were used for the statistical analysis further indicating similarity in head impact exposure for the comparative groups.

This technique is particularly useful in the analysis of heterogeneous tissue such as brain matter as it allows visual identification of regions with markedly higher or lower signal intensity and highlights regions of interest. Heatmaps assign a color to each superpixel based on DAB intensity along a spectrum with ranges defined by the user, which permits selective focus on higher or lower ends of staining intensity if desired. As long as the same range is used for a group of images, the relative intensities of stains can be directly compared within and between images. Importantly, the color assignment independent of the superpixel being positive or negative, and each superpixel is graded on a continuous scale. This allows visualization of subtle differences in intensities that may not be captured by the ordinal thresholds assigned for positivity. These heatmaps can then be exported as downsized JPEG images for quick reference, or as pieces of a larger image that can be externally stitched back together for a higher resolution image.

### Statistical analysis

Data were exported to Microsoft Excel and all statistical analysis was done using Stata 15. For behavioral and accelerometer analyses, the unit of comparison was the individual animal. To evaluate head impact exposure between collar and non-collar groups ( $n = 6-8/\text{group}$ ), Wilcoxon rank sum test were used compare peak linear acceleration and rotational velocity. Behavior scores were analyzed by Kruskal Wallis ( $n = 4/\text{group}$ ). For histopathological outcomes, the unit of comparison was individual sections ( $n = 20-80/\text{group}$ ). As multiple sections per animal per stain were analyzed, a negative binomial regression was employed, controlling for time, and clustered by individual animal to account for repeat measures across animals. Graphs were generated using Graphpad Prism 5.

## RESULTS

There were no deaths. Heart rate, respiratory rate, oxygen saturation, and core body temperature did not differ between groups ( $p > 0.05$ ). Both collar and non-collar injured animals showed a decrement in the clinical behavior score after injury, though there was no difference between groups (Fig. 3;  $p > 0.05$ ).

### Accelerometry

No differences were found in head impact exposure between the collar

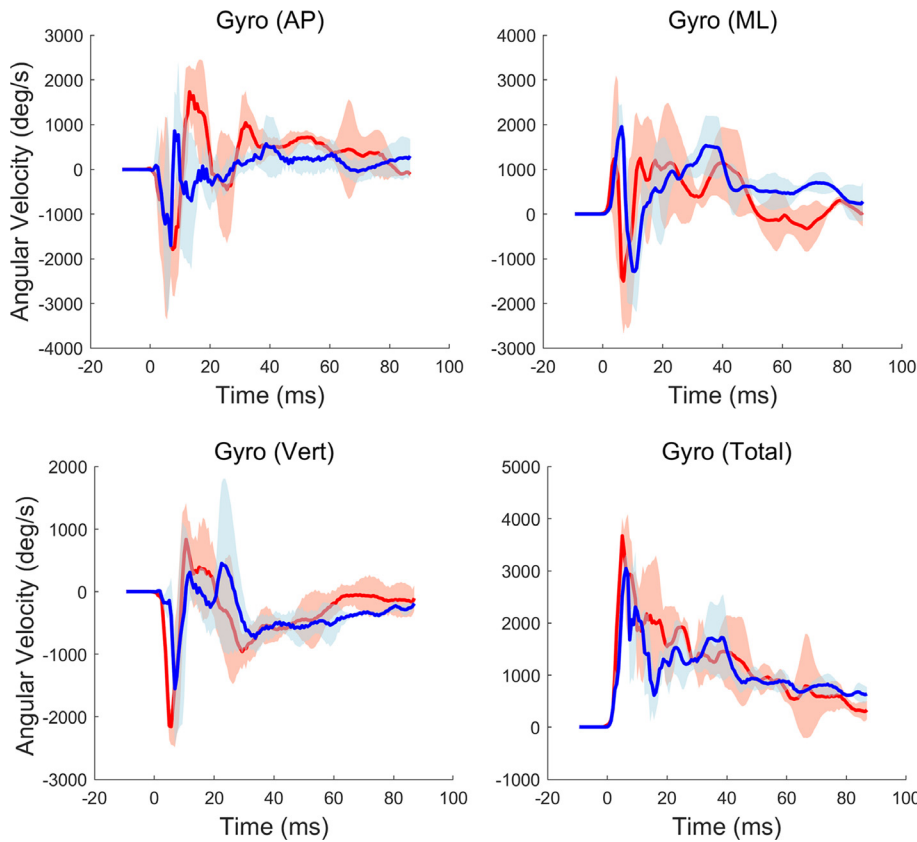


Fig. 4 (continued)

and non-collar groups. Specifically, temporal head impact exposure was characteristically similar, both temporally and structurally, for both linear acceleration and rotational velocity in all three planes of motion (Fig. 4). Peak values of linear acceleration and rotational velocity for both the collar and non-collar groups were all found to have come from a continuous distribution with the same median (Wilcoxon rank sum test; all  $p > 0.05$ ; Table 1).

**Gross dissection and histopathology**

Upon euthanasia and extraction of brains, no brain demonstrated evidence of gross cerebral hemorrhage or

dural rupture. There was no difference in brain mass between sham, non-collar animals, and collar animals ( $p > 0.05$ ).

Compared to sham animals, injured animals showed significant increases in AT8 staining across all thresholds ( $p < 0.001$  for all thresholds, Fig. 5). Relative to injured animals without collars, collared animals had significantly less AT8 staining at thresholds 2 and 3 ( $p = 0.03$  and  $p = 0.025$ , respectively). Injured animals without collar were different than sham at thresholds 2 and 3 ( $p < 0.01$ ). There was no difference between injured animals with collar and sham at thresholds 2 and 3 ( $p > 0.2$ ) and there was no effect of time from injury ( $p > 0.2$ ) across all thresholds.

Compared to sham animals, injured animals showed significant increases in IBA1 staining across all thresholds ( $p < 0.001$  for all thresholds, Fig. 6). Injured animals with collars demonstrated significantly less IBA1 staining at all thresholds ( $p = 0.008$ ,

$p = 0.039$ ,  $p = 0.044$  and  $p = 0.006$ , respectively for threshold 1, 2, 3 and all respectively, Fig. 6) relative to injured animals without collars. The effect of time was only significant at threshold 3 ( $p = 0.015$ ).

**Heatmaps**

Qualitative assessments of heatmaps for AT8 staining showed overall higher AT8 and IBA1 signal in the foremost two sections, approximately 15 mm and 25 mm from the front of the brain. AT8 increased most notably along the edges of the cortex, and surrounding sulci and ventricles. Importantly, AT8 supercellular tangles were

Table 1. Accelerometry Data.

Variable	mean_col	sd_col	mean_non	sd_non	p
Accel (AP)	117.2	16.5	85.2	38.8	0.400
Accel (ML)	46.3	9.0	31.2	2.0	0.114
Accel (Vert)	73.9	4.0	66.0	10.5	0.229
Accel (Total)	125.8	14.2	100.2	27.3	0.400
Gyro (AP)	2218.6	145.0	1477.1	762.0	0.114
Gyro (ML)	2260.3	74.9	2046.0	492.5	1.000
Gyro (Vert)	1162.9	260.2	1207.6	674.9	0.629
Gyro (Total)	3793.4	297.2	3253.4	96.8	0.057

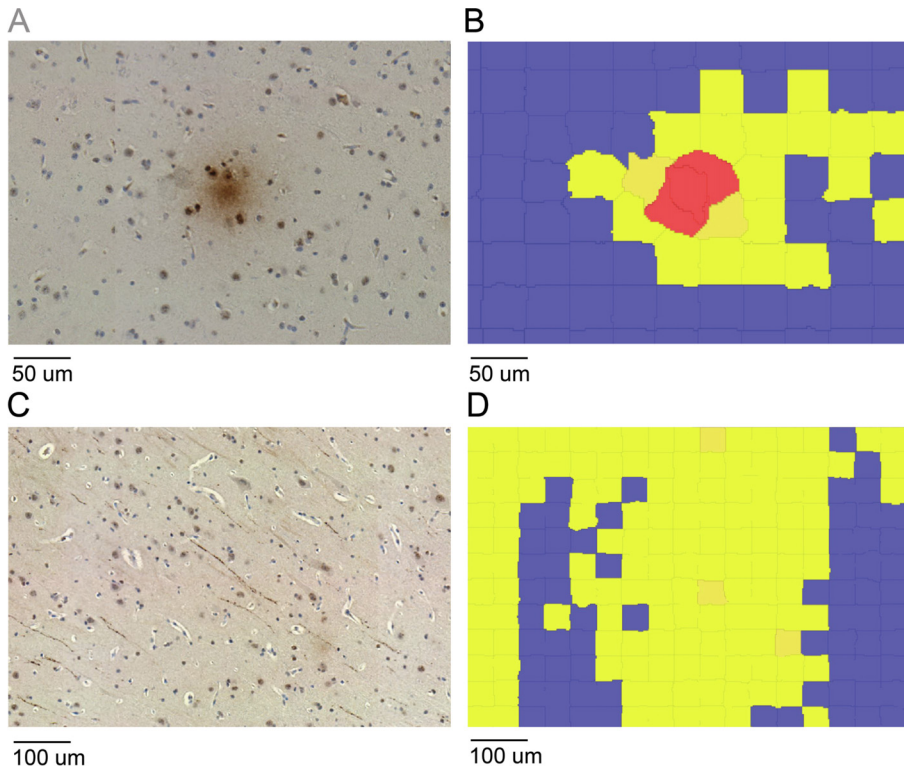


**Fig. 5.** Changes in phosphorylated tau in swine brain as a result of CHI and wearing of jugular compression collar during injury. **(A)** Example of a supercellular phosphorylated tau tangle staining positive for AT8. **(B)** Superpixels of AT8 positive tau tangle in A. Superpixels encompassing center of tangle are positive at the uppermost threshold of positivity (solid red), whereas superpixels surrounding the tangle are positive at the middle threshold (orange) and lowermost threshold (yellow) only. Negative superpixels are in blue. **(C)** Example of axons at edge of cortex staining positive for AT8. **(D)** Superpixels of AT8 positive axons in **(C)**. Superpixels containing a positive axon are positive only at the middle threshold (orange) or lowermost threshold (yellow). Negative superpixels are in blue. **(E)** Tau phosphorylation as measured by superpixel positivity at the three thresholds, and sum total of all positive superpixels. \*Indicates injured animals are significantly different from sham ( $p < 0.05$ ). \*\*Indicates collar animals are significantly different from non-collar animals ( $p < 0.05$ ). (For interpretation of the references to color in this figure legend, the reader is referred to the web version of this article.)

present in both injured and sham animals and were scattered throughout gray matter. These are visualized as red dots on their heatmaps. IBA1 signal was generally more apparent in WM and central brain structures than in gray matter or the cortex and did not appear to have consistent changes as a result of injury (Fig. 7). In contrast to the focal changes seen in AT8 histopathology, IBA1 signal globally changed as a result of injury (Fig. 7).

## DISCUSSION

In this study, we found that treatment with an innovative internal venous compression collar mitigates post-mTBI changes in AT8 and IBA1 in a porcine closed head injury model. Prior preclinical studies using murine models of closed head injury demonstrate the protective effects of jugular venous impedance on outcomes such as axonal injury, degenerative neurons and glial

activation (Smith et al., 2012; Turner et al., 2012). To our knowledge, this is the first study to demonstrate the protective effects of a jugular venous compression collar on histopathological outcomes in a gyrencephalic closed head injury model. A strength of the study is the automated quantification method allowing us to investigate diffuse, whole brain histopathological changes after injury. Importantly, our findings were not due to modifications in the biomechanics of injury in collar versus non collar animals as evidenced by similar accelerometry results between groups. These data have important clinical implications linking direct histopathological benefits to prior clinical trial efficacy in athletes engaged in high-risk collision and contact sports (Myer et al., 2016a,b; 2018; Yuan et al., 2017; 2018a,b). Further these data combined with prior reports support the use of IJV compression in those employed in the military where the risk of single and repetitive mTBI is significant and where widespread deployment of protective gear is feasible (Bonnette et al., 2018; Yuan et al., 2018b). In fact, given the repetitive and sometimes silent nature of head trauma in these settings, prophylactic treatment may be amongst the most effective strategies to reduce risk of short and long-term

microstructural changes associated with exposure to repetitive head trauma.

Our study demonstrates the effectiveness of a novel jugular compression collar device in mitigating phosphorylated tau accumulation (AT8) and microglial activation (IBA1) after single closed head injury. Both preclinical and clinical studies have suggested that tau phosphorylation is implicated in the causal pathway leading from repetitive mTBI to tauopathy, particularly as described in chronic traumatic encephalopathy (CTE) (Kondo et al., 2015; Turner et al., 2015). We therefore examined phosphorylation at pS202/pT205/pS208 residues (AT8), which has been previously shown to be a key phosphorylation pattern found in TBI related neurodegenerative diseases such as CTE (Mez et al., 2017). Our prior studies indicate that interventions targeting phosphorylated tau at early time points after injury prevents the development of CTE like pathology in murine close

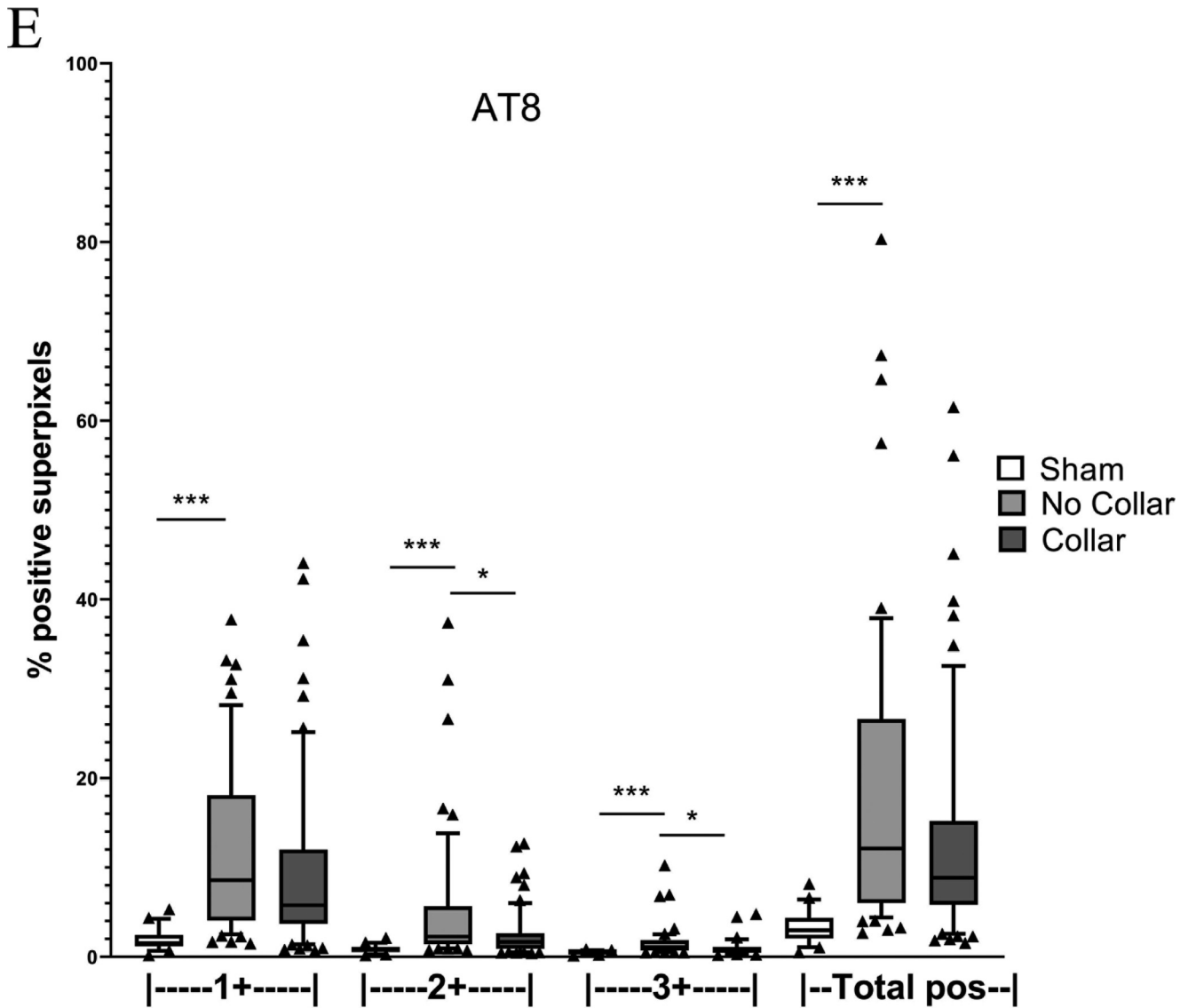


Fig. 5 (continued)

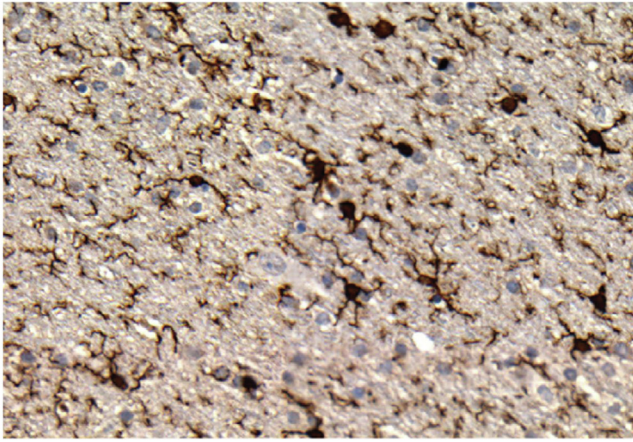
head injury models (Kondo et al., 2015). It will be vital to study whether collar treatment could result in long term mitigation of phosphorylated tau accumulation after single and repetitive mTBI.

Treatment with internal jugular venous compression also attenuated the increase in IBA1 reactivity (presumed microglial activation) after mTBI. The mechanism of this effect is uncertain but likely includes indirect protection through the reduction of triggers of microglial activation. For example, by decreasing the accumulation of phosphorylated tau after injury, internal jugular venous compression may also reduce the post-injury stimulus for microglial activation (Laurent et al., 2018). The durability of this response and association with long term outcomes was beyond the scope of the current study but will need to be addressed in future efforts.

These tissue level findings are important correlates to clinical studies that have reported the protective effects of

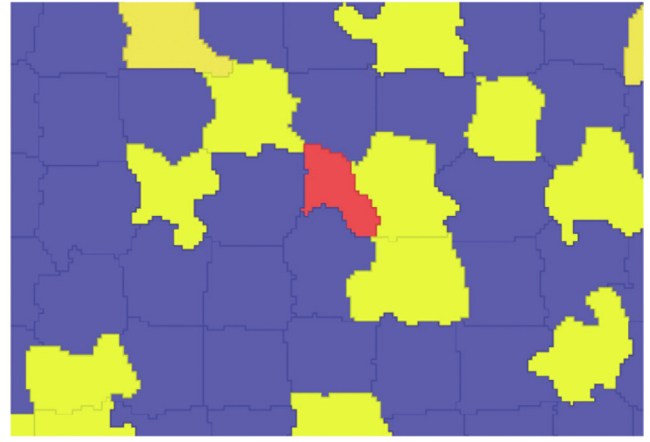
internal jugular venous compression against microstructural injury after head trauma exposure. Indeed, the clinical literature has suggested that internal jugular venous compression prevents alterations to WM integrity and brain network neurophysiology following head impact exposure (Myer et al., 2016a). Correlating these imaging biomarkers with fluid biomarkers of injury, such as serum tau or neurofilament light chain, would further substantiate the protective effects of this intervention. However, it is notable that the protective effects of jugular venous compression has not been proven in the setting of a single mTBI event. Moreover, we did not find any changes in symptoms in collared versus non collared animals. Whether or not collar treatment might mitigate functional outcomes after single mTBI was not assessed in the current study. The findings in our study warrant further work to support translation of results to this common clinical scenario.

A



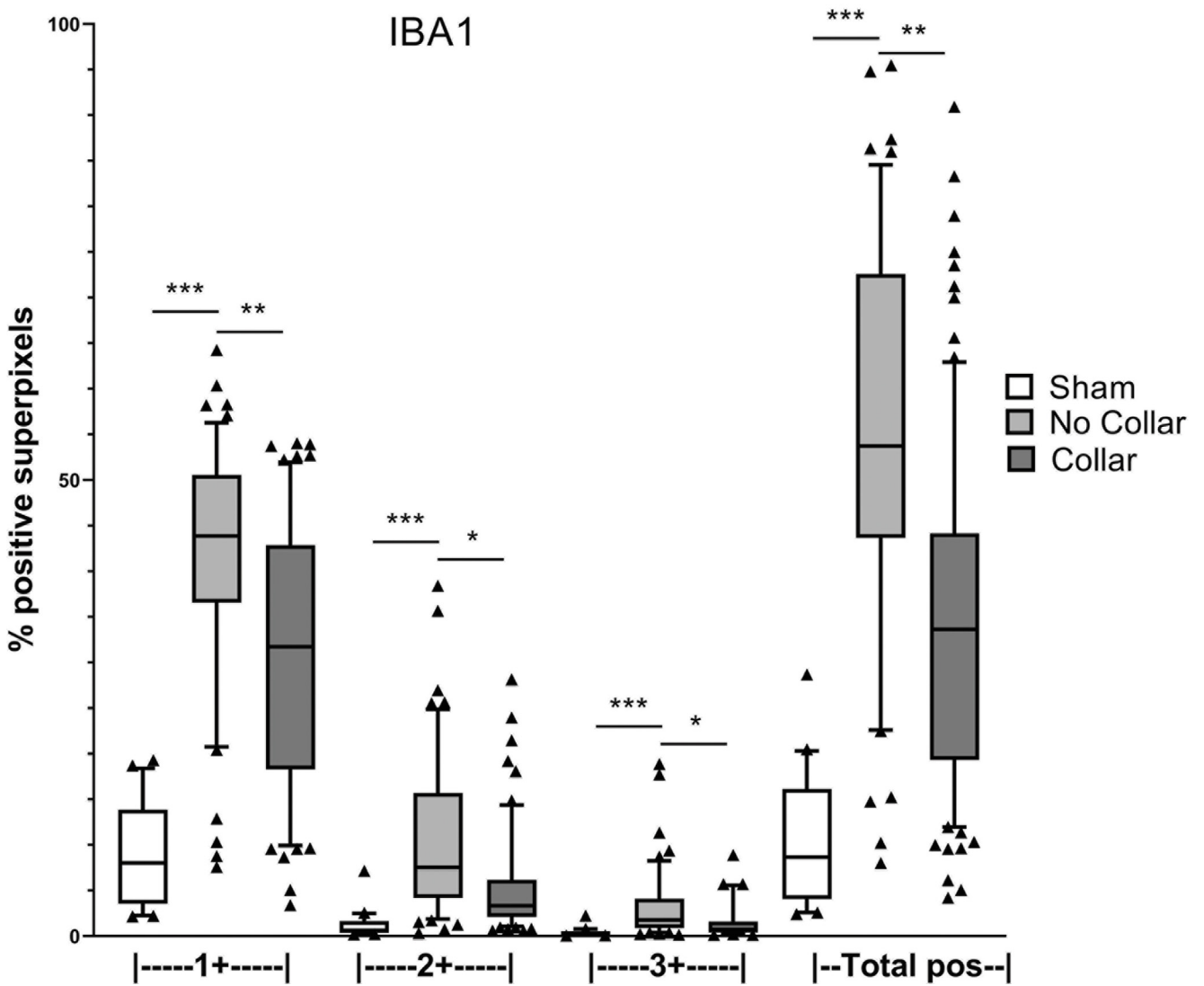
50  $\mu$ m

B



50  $\mu$ m

C



This study has several important limitations. First, we evaluated the effect of collar treatment on a single mTBI injury. It is uncertain whether collar treatment would demonstrate similar tissue level protection in the setting of repetitive injury, though the clinical literature suggests a beneficial effect of internal jugular venous compression in the setting of exposure to repetitive head trauma (Myer et al., 2016b; Yuan et al., 2017, 2018a). Second, the collar was applied for a brief duration, immediately before injury and removed immediately after injury. It will be important to investigate how duration of collar placement affects outcomes after injury. Third, we did not compare tissue level changes to imaging biomarkers in the current study, though we plan to investigate these correlations in future studies. This will be important as tissue level changes can only indirectly be assayed in clinical mTBI, through the use of imaging or fluid biomarkers. Understanding whether imaging biomarkers predict tissue level changes, particularly those associated with long-term neurodegenerative sequelae, is a vital step for clinicians managing patients exposed to head trauma and repetitive head trauma. Fourth, we evaluated treatment at subacute but not chronic time points after injury. As the prevention of neurodegenerative changes is of primary interest, especially in the case of collision sport athletes and those in the military, long-term studies are needed to investigate the durability of collar protection. Fifth, we investigated a limited set of histopathological outcomes, limited to those most relevant to sport related TBI and CTE. Sixth, we did not have sufficient power to investigate functional outcomes in collar versus non collar animals in the current study. Finally, while the use of accelerometry to ensure standardization of head trauma between groups strengthens the between group comparisons, the authors acknowledge that accelerometry cannot provide a direct measure of brain motion or load during the application of head impact. Future studies that with MR elastography or dynamic imaging or Finite Element Analysis may further elucidate the mechanistic response of the brain to the collar application that underlies the protective effects noted in the current pilot investigation.

The results of the current study indicate that internal jugular venous compression protects against tau phosphorylation and microglial activation after a single closed head injury in swine. To our knowledge, this is

the first study to directly address prophylactic treatment for mTBI-induced histopathological changes in a swine close head injury model, relevant to athletes and veterans who are at high risk of closed head mTBI. While an increasing body of literature suggest that jugular venous impedance mitigates neuroimaging biomarkers of injury after exposure to head trauma, the protective effects in preventing imaging and/or histopathological changes after single mTBI have not been fully characterized. However, current results indicate a protective effect of collar treatment on direct measures of brain health following traumatic head impact. Future work that links the histopathologic injury to imaging biomarkers showing similar of internal jugular vein (IJV) compression collar efficacy in clinical trials may further substantiate this novel approach as a viable solution to protect the brain from external trauma.

## DISCLOSURES

Dr. Meehan receives royalties from ABC-Clio publishing for the sale of his book, *Kids, Sports, and Concussion: A guide for coaches and parents*, and from Springer International for the book *Head and Neck Injuries in Young Athlete* and from royalties from Wolters Kluwer for working as an author for *UpToDate*. He is under contract with ABC-Clio publishing for a future book entitled, *Concussions*. Gregory D. Myer has consulted with Q30 Innovations to support application to the US Food and Drug Administration but has no financial interest in the commercialization of the Q-Collar. Dr. Myer also received current and ongoing funding Support from National Institutes of Health/NIAMS Grants U01AR067997, R01 AR070474, R01 AR056259-01, and industry sponsored research funding related to brain injury prevention and assessment with Q30 Innovations, LLC and EIMinda, Ltd. Dr. Myer also receives author royalties from Human Kinetics and Wolters Kluwer. Dr. Myer is an inventor of biofeedback technologies (2017 Non Provisional Patent Pending- Augmented and Virtual reality for Sport Performance and Injury Prevention Application filed 11/10/2016 (62/420119), Software Copyrighted.) designed to enhance rehabilitation and prevent injuries and has potential for future licensing royalties.

**Fig. 6.** Changes in microglial activation in swine brain as assessed by IBA1 signal of CHI and wearing of jugular compression collar during injury. **(A)** Example of IBA1 positive, activated microglia in swine cortex, with multiple microprocesses and relatively large cell bodies. **(B)** Superpixels of microglia in **(A)**. The superpixel encompassing the large cell body with multiple microprocesses (center, red) is the only one positive at the uppermost threshold. Superpixels encompassing slightly smaller cell bodies and/or ones with fewer microprocesses are positive at either the lowermost threshold (yellow) or middle threshold (orange). Superpixels with few microprocesses and no cell bodies are predominantly negative (blue). **(C)** Microglial activation as measured by superpixel positivity at the three thresholds, and sum total of all positive superpixels. DPI stands for days post injury. \*Indicates injured animals are significantly different from sham ( $p < 0.05$ ). \*\*Indicates collar animals are significantly different from non-collar animals ( $p < 0.05$ ). \*\*\*Indicates three days post injury animals are significantly different from 23 days post injury animals ( $p < 0.05$ ). Error bars are  $\pm$  standard error of the mean. (For interpretation of the references to color in this figure legend, the reader is referred to the web version of this article.)

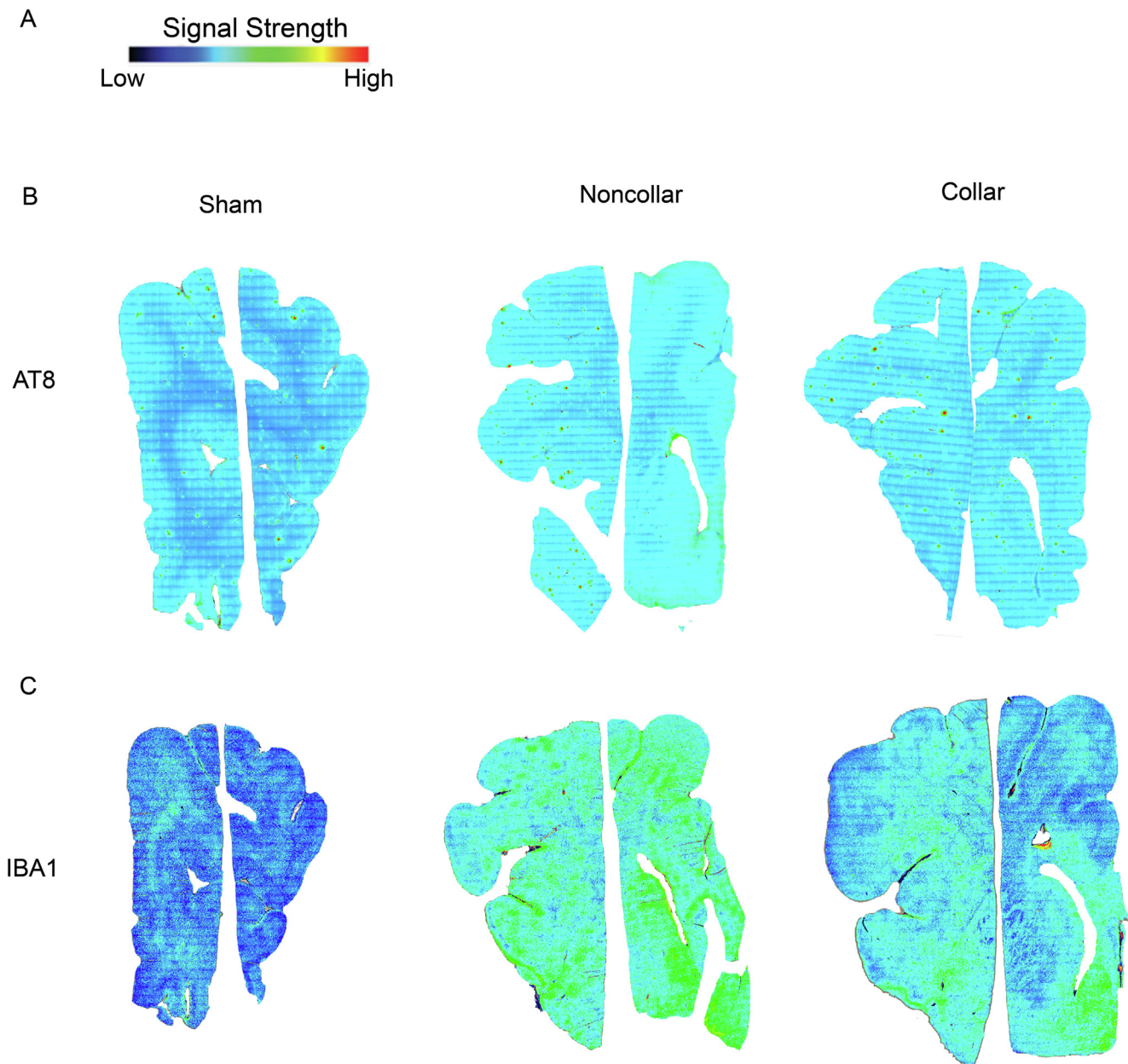


**Fig. 7.** Heatmaps of AT8 signal for tau phosphorylation and IBA1 signal for microglial activation. **(A)** Color representation of relative superpixel positivity. **(B)** AT8 signal in sham, injured animals without collar (noncollar), and injured animals with collar (collar). Signal in sham animals is overall lower, and there are markedly fewer supercellular tau tangles (visible in red) than in noncollar or collar animals, although these tangles are not entirely absent. Noncollar animals show higher AT8 signal in particular along the edges of cortex and surrounding sulci. Collar animals showed overall reduced signal in comparison to noncollar, with notably fewer supercellular tau tangles and fewer strongly positive regions. **(C)** IBA1 signal in sham, injured animals without collar (noncollar), and injured animals with collar (collar). Signal in sham animals is overall lower than both noncollar and collar animals. No specific regions of markedly different stain intensity were obviously apparent; rather, IBA1 signal changed globally as a result of injury and/or collar. Error bars are  $\pm$  standard error of the mean. (For interpretation of the references to color in this figure legend, the reader is referred to the web version of this article.)

### FUNDING

This work was supported in part by funding from the CHB IDDRC and by philanthropic support from the National Hockey League Alumni Association through the Corey

C. Griffin Pro-Am Tournament and the National Football League. Q30 Sports Innovations, LLC funded the development of the swine jugular compression collar to Priority Designs and provided funding for portions of this project.

## REFERENCES

- Benson BW, Hamilton GM, Meeuwisse WH, McCrory P, Dvorak J (2009) Is protective equipment useful in preventing concussion? A systematic review of the literature. *Br J Sports Med* 43(Suppl. 1): i56–67.
- Bonnette S, Diekfuss JA, Kiefer AW, Riley MA, Barber Foss KD, Thomas S, DiCesare CA, Yuan W, Dudley J, Reches A, Myer GD (2018) A jugular vein compression collar prevents alterations of endogenous electrocortical dynamics following blast exposure during special weapons and tactical (SWAT) breacher training. *Exp Brain Res* 236(10):2691–2701.
- Browne KD, Chen XH, Meaney DF, Smith DH (2011) Mild traumatic brain injury and diffuse axonal injury in swine. *J Neurotrauma* 28(9):1747–1755.
- Gilland O, Chin F, Anderson WB, Nelson JR (1969) A cinemeyelographic study of cerebrospinal fluid dynamics. *Am J Roentgenol Radium Ther Nucl Med* 106(2):369–375.
- Guskiewicz KM, Mihalik JP (2011) Biomechanics of sport concussion: quest for the elusive injury threshold. *Exerc Sport Sci Rev* 39(1):4–11.
- Koerte IK, Kaufmann D, Hartl E, Bouix S, Pasternak O, Kubicki M, Rauscher A, Li DK, Dadachanji SB, Taunton JA, Forwell LA, Johnson AM, Echlin PS, Shenton ME (2012) A prospective study of physician-observed concussion during a varsity university hockey season: white matter integrity in ice hockey players. Part 3 of 4. *Neurosurg Focus* 33(6). E3: 1–7.
- Kondo A, Shahpasand K, Mannix R, Qiu J, Moncaster J, Chen CH, Yao Y, Lin YM, Driver JA, Sun Y, Wei S, Luo ML, Albayram O, Huang P, Rotenberg A, Ryo A, Goldstein LE, Pascual-Leone A, McKee AC, Meehan W, Zhou XZ, Lu KP (2015) Antibody against early driver of neurodegeneration cis P-tau blocks brain injury and tauopathy. *Nature* 523(7561):431–436.
- Laurent C, Buee L, Blum D (2018) Tau and neuroinflammation: what impact for Alzheimer's Disease and Tauopathies? *Biomed J* 41(1):21–33.
- Margulies S, Coats B (2013) Experimental injury biomechanics of the pediatric head and brain. In: *Pediatric injury biomechanics*. Springer. p. 157–189.
- McKee AC, Cantu RC, Nowinski CJ, Hedley-Whyte ET, Gavett BE, Budson AE, Santini VE, Lee HS, Kubilus CA, Stern RA (2009) Chronic traumatic encephalopathy in athletes: progressive tauopathy after repetitive head injury. *J Neuropathol Exp Neurol* 68(7):709–735.
- McKee AC, Stern RA, Nowinski CJ, Stein TD, Alvarez VE, Daneshvar DH, Lee HS, Wojtowicz SM, Hall G, Baugh CM, Riley DO, Kubilus CA, Cormier KA, Jacobs MA, Martin BR, Abraham CR, Ikezu T, Reichard RR, Wolozin BL, Budson AE, Goldstein LE, Kowall NW, Cantu RC (2013) The spectrum of disease in chronic traumatic encephalopathy. *Brain* 136(Pt 1):43–64.
- Mez J, Daneshvar DH, Kiernan PT, Abdolmohammadi B, Alvarez VE, Huber BR, Alosco ML, Solomon TM, Nowinski CJ, McHale L, Cormier KA, Kubilus CA, Martin BM, Murphy L, Baugh CM, Montenigro PH, Chaisson CE, Tripodis Y, Kowall NW, Weuve J, McClean MD, Cantu RC, Goldstein LE, Katz DI, Stern RA, Stein TD, McKee AC (2017) Clinicopathological evaluation of chronic traumatic encephalopathy in players of American football. *JAMA* 318(4):360–370.
- Myer GD, Barber Foss K, Thomas S, Galloway R, DiCesare CA, Dudley J, Gadd B, Leach J, Smith D, Gubanich P, Meehan 3rd WP, Altaye M, Lavin P, Yuan W (2018) Altered brain microstructure in association with repetitive subconcussive head impacts and the potential protective effect of jugular vein compression: a longitudinal study of female soccer athletes. *Br J Sports Med*.
- Myer GD, Yuan W, Barber Foss KD, Smith D, Altaye M, Reches A, Leach J, Kiefer AW, Khoury JC, Weiss M, Thomas S, Dicesare C, Adams J, Gubanich PJ, Geva A, Clark JF, Meehan 3rd WP, Mihalik JP, Krueger D (2016a) The effects of external jugular compression applied during head impact exposure on longitudinal changes in brain neuroanatomical and neurophysiological biomarkers: a preliminary investigation. *Front Neurol* 7:74.
- Myer GD, Yuan W, Barber Foss KD, Thomas S, Smith D, Leach J, Kiefer AW, Dicesare C, Adams J, Gubanich PJ, Kitchen K, Schneider DK, Braswell D, Krueger D, Altaye M (2016b) Analysis of head impact exposure and brain microstructure response in a season-long application of a jugular vein compression collar: a prospective, neuroimaging investigation in American football. *Br J Sports Med* 50(20):1276–1285.
- Noy S, Krawitz S, Del Bigio MR (2016) Chronic traumatic encephalopathy-like abnormalities in a routine neuropathology service. *J Neuropathol Exp Neurol*.
- Omalu BI, DeKosky ST, Hamilton RL, Minster RL, Kamboh MI, Shakir AM, Wecht CH (2006) Chronic traumatic encephalopathy in a national football league player: part II. *Neurosurgery* 59(5):1086–1092. discussion 1092–1083.
- Omalu BI, DeKosky ST, Minster RL, Kamboh MI, Hamilton RL, Wecht CH (2005) Chronic traumatic encephalopathy in a National Football League player. *Neurosurgery* 57(1):128–134. discussion 128–134.
- Schneider DK, Galloway R, Bazarian J, Diekfuss JA, Dudley J, Leach J, Mannix R, Talavage TM, Yuan W, Myer GD (2019) Diffusion tensor imaging in athletes sustaining repetitive head impacts: a systematic review of prospective studies. *J Neurotrauma*.
- Schneider DK, Grandhi RK, Bansal P, Kuntz GE, Webster KE, Logan K, Barber Foss KD, Myer GD (2017) Current state of concussion prevention strategies: a systematic review and meta-analysis of prospective, controlled studies. *Br J Sports Med* 51(20):1473–1482.
- Smith DW, Bailes JE, Fisher JA, Robles J, Turner RC, Mills JD (2012) Internal jugular vein compression mitigates traumatic axonal injury in a rat model by reducing the intracranial slosh effect. *Neurosurgery* 70(3):740–746.
- Stern RA, Riley DO, Daneshvar DH, Nowinski CJ, Cantu RC, McKee AC (2011) Long-term consequences of repetitive brain trauma: chronic traumatic encephalopathy. *PM R* 3(10 Suppl 2): S460–467.
- Turner RC, Lucke-Wold BP, Logsdon AF, Robson MJ, Dashnaw ML, Huang JH, Smith KE, Huber JD, Rosen CL, Petraglia AL (2015) The quest to model chronic traumatic encephalopathy: a multiple model and injury paradigm experience. *Front Neurol* 6:222.
- Turner RC, Naser ZJ, Bailes JE, Smith DW, Fisher JA, Rosen CL (2012) Effect of slosh mitigation on histologic markers of traumatic brain injury: laboratory investigation. *J Neurosurg* 117(6):1110–1118.
- Yuan W, Barber Foss KD, Dudley J, Thomas S, Galloway R, DiCesare C, Leach J, Scheifele P, Farina M, Valencia G, Smith D, Altaye M, Rhea CK, Talavage T, Myer GD (2018a) Impact of low-level blast exposure on brain function after a one-day tactile training and the ameliorating effect of a jugular vein compression neck collar device. *J Neurotrauma*.
- Yuan W, Dudley J, Barber Foss KD, Ellis JD, Thomas S, Galloway RT, DiCesare CA, Leach JL, Adams J, Maloney T, Gadd B, Smith D, Epstein JN, Grooms DR, Logan K, Howell DR, Altaye M, Myer GD (2018b) Mild jugular compression collar ameliorated changes in brain activation of working memory after one soccer season in female high school athletes. *J Neurotrauma* 35(11):1248–1259.
- Yuan W, Leach J, Maloney T, Altaye M, Smith D, Gubanich PJ, Barber Foss KD, Thomas S, DiCesare CA, Kiefer AW, Myer GD (2017) Neck collar with mild jugular vein compression ameliorates brain activation changes during a working memory task after a season of high school football. *J Neurotrauma* 34(16):2432–2444.
- Zemek R, Barrowman N, Freedman SB, Gravel J, Gagnon I, McGahern C, Aglipay M, Sangha G, Boutis K, Beer D, Craig W, Burns E, Farion KJ, Mikrogianakis A, Barlow K, Dubrovsky AS, Meeuwisse W, Gioia G, Meehan 3rd WP, Beauchamp MH, Kamil Y, Grool AM, Hoshizaki B, Anderson P, Brooks BL, Yeates KO, Vassilyadi M, Klassen T, Keightley M, Richer L, DeMatteo C,

Osmond, T. Pediatric Emergency Research Canada Concussion (2016) Clinical risk score for persistent postconcussion symptoms among children with acute concussion in the ED. *JAMA* 315 (10):1014–1025.

## APPENDIX A. SUPPLEMENTARY DATA

Supplementary data to this article can be found online at <https://doi.org/10.1016/j.neuroscience.2020.04.009>.

*(Received 12 March 2020, Accepted 5 April 2020)*  
*(Available online 10 April 2020)*